Progress In Electromagnetics Research M, Vol. 11, 65–77, 2010

A WIDE BAND ANTENNA FOR MULTI-CONSTELLATION GNSS AND AUGMENTATION SYSTEMS

A. Kumar

Defence Electronic Research Laboratory
Kesavgiri Post, Hyderabad 500 005, India

A. D. Sarma

R & T Unit for Navigational Electronics
Osmania University
Hyderabad 500 007, India

A. K. Mondal

Defence Electronic Research Laboratory
Kesavgiri Post, Hyderabad 500 005, India

K. Yedukondalu

Department of ECE
Bhoj Reddy Engineering College for Women
Saidabad, Hyderabad, India

Abstract—Local Area Augmentation System (LAAS) based on multi-constellation GNSS can provide improved accuracy, availability and integrity needed to support all weather category II and III precision approach landing of aircraft. In order to receive satellite signals of GNSS, an antenna working over wide frequency band and high phase center stability is preferred. Commonly used antennas like crossed dipoles, patch etc. are inherently narrow band. This paper describes the design and development of half-cardioid shaped dual arm, wide band printed circuit antenna. The antenna has low VSWR of $< 3 : 1$, a stable phase center and good right hand circularly polarized radiation patterns covering full L-band frequencies. The simulated and measured results compare well. This compact antenna can also be used on ground, ship and airborne platforms to receive signals from multiple GNSS satellites above the horizon.

Corresponding author: K. Yedukondalu (kyedukondalu@gmail.com).

1. INTRODUCTION

In order to improve the accuracy, reliability and/or availability of a stand-alone satellite based navigation and positioning systems, differential navigation systems are being proposed. These are mostly Satellite Based Augmentation system (SBAS) and Ground Based Augmentation system (GBAS). These systems correct the bias errors of the location with respect to a known reference position through additional differential corrections. This information is provided from geostationary communication satellites (in the case of SBAS) or ground reference stations (in the case of GBAS). Local Area Augmentation System (LAAS) is a GBAS and is being developed by the Federal Aviation Administration (FAA). Other countries like India are expected to implement such a system in the near future. This is being aimed at providing category II and III precision approach and landing of aircraft [1]. For such high precision requirement large numbers of satellites in space having wider angular separation between them is essential.

In the coming years more than 60 satellites with multiple ranging signals will be available from Global Navigation Satellite Systems (GNSSs) consisting of the modernized American GPS (L2C and L5), updated GLONASS (L1 and L2), European Galileo (E5a, E5b, and E6) and other regional systems [2, 3]. Therefore, the future navigation receivers should be capable of working for all the GNSS frequencies. This interoperability between the GNSS systems will help in overcoming some of the shortfalls of individual navigation systems such as service guarantees, integrity monitoring, and improved service performance [4].

If individual antennas are employed for reception of each frequency of GNSS signals, it will be quite costly in addition to increased complexity of the complete system. Therefore, this necessitates the development of multi-frequency or wide frequency band antennas. The antenna for such applications should also have circularly polarized wide angle radiation pattern and a stable phase center. It is difficult to design and develop such a high performance antenna that covers all the required frequency bands of GNSS. Presently satellite navigation receivers are using various types of antennas such as helical antennas, crossed dipoles, patch antennas etc [5–7]. These antennas cover very narrow frequency bandwidth and cannot be used for GNSS based SBAS or LAAS applications. The popular printed circuit patch antennas are widely used for single, dual and triple-frequency operation for GPS system [8–11]. For achieving circular polarisation and multi frequency operation from the same

antenna, one has to employ complex feed networks, hybrids, pin diodes, Micro Electomechanical Switches (MEMS) or a combination of these techniques [12, 13]. These antennas are expensive, difficult to design and do not meet the complete requirement of wideband GNSS, pseudolite based navigation system and augmentation systems. So the necessity of an inexpensive wide band antenna design still exists. It has been established that if an antenna structure is characterized by ratio or angles, they show broadband performance. Antennas like equiangular spiral, Archimedean spiral, conical helix etc. come under this category [14, 15]. This concept has been implemented in this work for the design of a novel half-cardioid shaped dual arm printed antenna for covering the entire L-band for GNSS applications.

2.1. Antenna Design

The basic configuration of the wide band, printed circuit antenna for GNSS based LAAS application is shown in Fig. 1. The antenna has two metallic arms each having a cardioid shape. A cardioid can be defined as the trace of a point on a circle that rolls around a fixed circle of the same size without slipping. The antenna arm geometry is generated by a cardioid curve defined by the following equation [16].

$$R = a * (1 \pm \cos\theta) \quad (0 < \theta < 2\pi) \tag{1}$$

where 'R' is the radius vector of the curve, 'θ' is the angular position and 'a' is the diameter of the cardioids segment from cusp to vertex. The parameter 'a' determines the size of the cardioid.

The values of θ in Eq. (1) are limited between 0 to π to get only half curve of the cardioid which forms the arm of the antenna. This antenna consists of two oppositely placed arms. If one arm of the antenna is generated by selecting $(1 + \cos\theta)$ in the equation then the

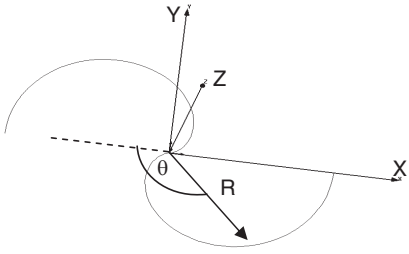

Figure 1. Half cardioid curved dual arm antenna configuration.

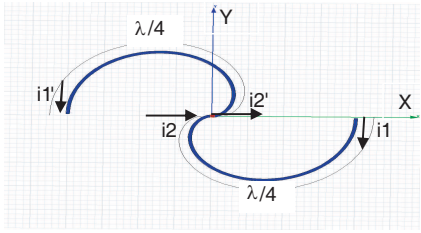

Figure 2. Orientation of current on the cardioid arms.

other arm is generated by selecting $(1 - \cos\theta)$. The width of the arms is decided by growth factor 'g' defined as

$$g = a_1/a_2 \tag{2}$$

where a_1 and a_2 are two different values for 'a'. Thus the design equations for the antenna arms are given as

$$R_1 = a_1 * (1 \pm \cos\theta) \text{ and } R_2 = a_2 * (1 \pm \cos\theta) \quad (0 < \theta < \pi) \tag{3}$$

where, R_1 and R_2 are the outer and inner radii vectors of the outer and inner curves of the arm, respectively.

Integrating Eq. (3) over 0 to π one can get the length of each arm as $4a$ which is taken as $\lambda/4$, similar to the case of a dipole. Here, $\lambda = \lambda_0/\checkmark\varepsilon_r$ where λ_0 is free space wavelength and ε_r is relative dielectric constant of the substrate. The maximum size of the antenna along X-axis will be $\lambda/4$ which is less than the size of cavity backed Archmedian spiral antenna, i.e., λ/π. As the structure is solely defined by angle this will give frequency independent characteristics [15, 17, 18].

In this design, circular polarization is achieved due to orientation of the current "i_2" and "i_2'" along horizontal X-axis and "i_1" and "i_1'" along vertical Y-axis (Fig. 2). The current "i_1" and "i_2" and "i_1'" and "i_2'" are oriented and separated in such a way to provide the necessary phase difference of 90° in time and space to give circular polarisation. Also, the two cordioid arms are excited 180° out of phase making the corresponding currents "i_1, i_1'" and "i_2, i_2'" in phase. This arrangement facilitates maximum radiation along the axis of the antenna. Anti clockwise orientation of the curved arms will give right hand circular polarization while a clockwise direction will give left hand circular polarization.

From above, it is observed that this antenna is more compact than spirals with similar characteristics. Thus, it can be used as radiating element to fit within the inter-element spacing requirement for wide angle scanning array. From the design, it is also observed that this antenna geometry differs from that of the conventional spiral antenna as it does not require multiple turns as for the spiral arms. The ends of the two arms are truncated to produce the smallest physical antenna for a given lower resonant frequency.

2.2. Simulation Analysis

In order to predict the antenna performance in terms of the input impedance and radiation patterns, the design parameter 'g' was optimized through extensive Finite-Element-Model (FEM) based simulations. The commercial High-Frequency Structure Simulator (HFSS V10.1) software (M/s Ansoft Corp., Pittsburgh, PA) was used

for the analysis [19]. The antenna structure (Fig. 3) was modeled using Eq. (3) and positioned on a 0.254 mm thick RT/Duroide 5880 substrate of dielectric constant 2.2. Initially the antenna feed point gap was optimized for minimum impedance variation over the required frequency band of 1 to 2 GHz. The antenna shows impedance variation from 85 Ω to 166 Ω over the band. This variation depends upon the growth factor 'g' for a fixed 'R' value. The growth factor 'g' has been varied from 1 to 2 in steps of 0.2 for achieving optimum geometry. The simulated impedance variation over the frequency band for $g = 1.8$ is shown in Smith chart (Fig. 4). The corresponding variation in Return Loss of the antenna for various growth factors is presented in Fig. 5.

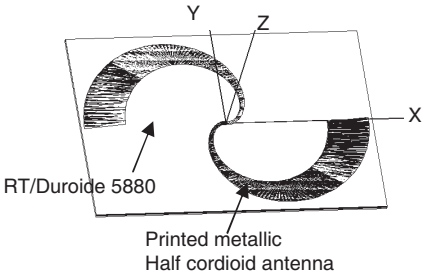

Figure 3. Antenna structure schematic for simulation studies.

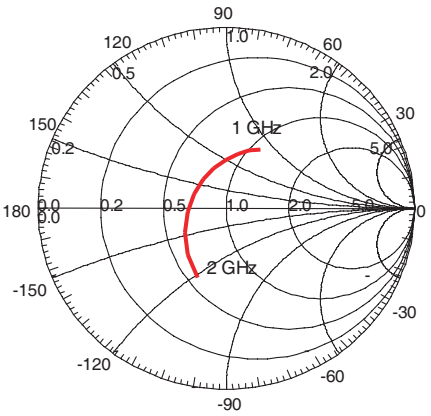

Figure 4. Simulated impedance variation over 1 to 2 GHz.

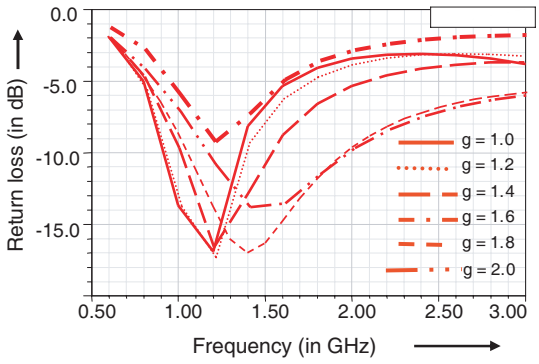

Figure 5. Simulated return loss for different growth factors (g) of the cardioid arms.

It is observed from these plots that the antenna has lowest return loss around center frequencies of 1.4 GHz to 1.6 GHz. Also, it is noticed that with the increase in growth factor, return loss improves towards higher frequency end indicating that the antenna can operate over a wider frequency band. The return loss between 1–2 GHz is better than −8 dB.

An optimum gap of 0.5 mm is provided along the x-axis at the center of the antenna for feeding. The simulated radiation patterns of the antenna for a growth factor $g = 1.8$, at various frequencies (1, 1.5 and 2 GHz) are shown in Fig. 6. It is observed that the patterns are bidirectional; as no cavity is used in simulation. It also shows wide beams for both vertical and horizontal polarizations for $\phi = 0°$ (X-Z plane) and $\phi = 90°$ (Y-Z plane). The 3 dB beam width is better than 100° for all the frequencies, in both polarizations and both planes. The difference between the horizontal and vertical polarization patterns in

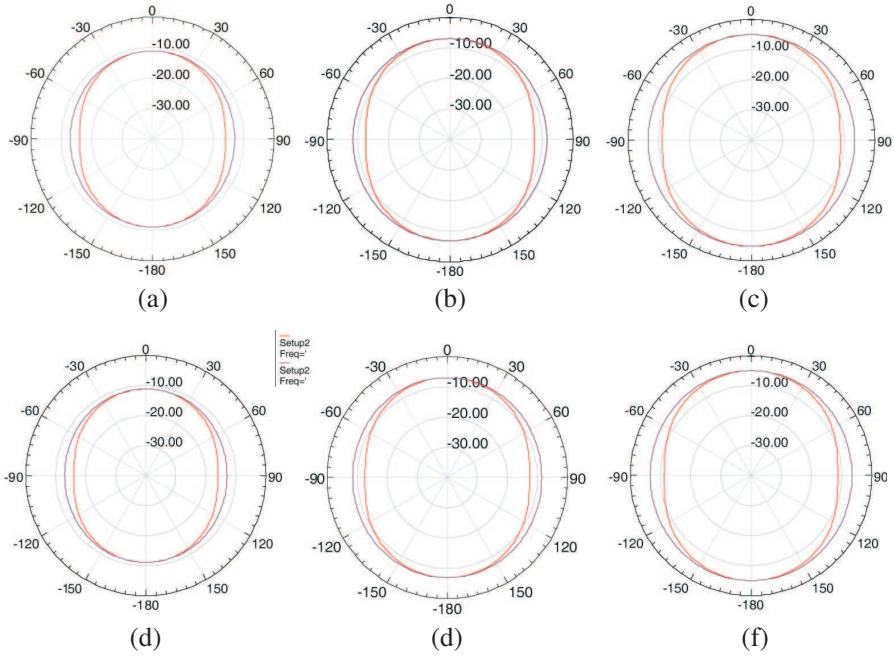

Figure 6. Simulated radiation patterns of the antenna without cavity ($\phi = 0°$ red, $\phi = 90°$ gray). (a) Freq = 1.0 GHz, E_θ ($\phi = 0°$), (b) Freq = 1.5 GHz, E_θ ($\phi = 0°$), (c) Freq = 2 GHz, E_θ ($\phi = 0°$), (d) Freq = 1 GHz, E_θ ($\phi = 90°$), (e) Freq = 1.5 GHz, E_θ ($\phi = 90°$), (f) Freq = 2 GHz, E_θ ($\phi = 90°$).

the principal planes is less than 3 dB indicating a very low deviation from circular polarization over wide angular coverage and over the entire operating band (Figs. 6(a)–6(f)).

3. PHASE CENTER OF THE ANTENNA

Broadband or multiband antennas being developed for covering GNSS services will have large dimension along the z axis of the radiating structure. This is apparent for various stacked patch antennas proposed for dual or triple frequencies GPS receivers [10, 11, 13]. Such antennas will excite larger current at the periphery of the antenna, which may cause much larger movement of phase center. It may not be practically possible to compensate or correct such phase center movement at the receiver. The proposed half-cardioid shaped dual arm antenna has advantage over the stacked patch type of antennas. It has planar structure, similar to that of planar spiral. The surface current distribution on the arms at the highest frequency is presented in Fig. 7. The surface current distribution was simulated over the full frequency band with an interval of 0.2 GHz and found to be symmetrical on both the arms. It can be easily observed that the current is symmetrical on both the arms and its strength varies from maximum at the center of the antenna and decreases out at the arm ends. Thus complete radiation takes place before the traveling wave reaches the outer end of the arm. The design symmetry of its radiating arms and position of the feed about the antenna central vertical axis also ensures a more stable phase center with angular and frequency variations. This clearly indicates that the antenna has a stable phase center which is very essential for GNSS applications.

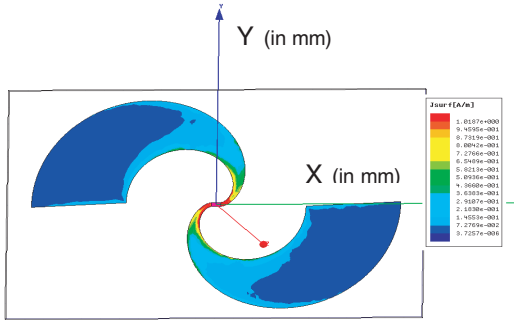

Figure 7. Surface current distribution on cadioid arms of the antenna at 2 GHz.

4.1. Fabrication and Assembly

The dual arms of the antenna were printed using photolithography technique on one side of RT-duroid 5880 copper clad dielectric substrate. The other side was completely etched to remove the copper cladding. The substrate selected is 0.254 mm thick and has a relative dielectric constant of 2.2. The two printed arms of the antenna form a balanced structure with maximum impedance varying between 85 to 166 ohms. Since it has to be fed through coaxial input connector which is an unbalanced line, it becomes essential to design and integrate a suitable 'balun'. This 'balun' will provide impedance matching and transformation between balanced antenna arms to unbalanced input coaxial transmission line.

4.2. Balun Configuration

The transition from unbalanced coax input to balanced twin arms antenna shown in Fig. 3 is accomplished by using a wideband printed balun. Here, the balun employed is a 1 : 3 Chebyshev type microstrip impedance transformer together with a two wire line. This twin wire line connects the antenna feed point with high impedance end of the transformer. It offers wideband matching from 50 ohms coaxial line to antenna. The Chebyshev transformer line was printed on one side of a $50 \times 10 \times 0.785$ mm RT/Duroid copper clad substrate having a relative dielectric constant (ϵ_r) 2.2 with other side as ground plane.

4.3. Cavity for Unidirectional Radiation from Cardioid Arms Antenna

The planar cardioid arms antenna has bidirectional radiation patterns perpendicular to the plane of the antenna as expected for such planar antennas [17, 18]. This phenomenon has been observed in the simulation studies as well (Fig. 6). However, a unidirectional pattern is preferred in order to receive signals from one direction only. Thus, to obtain unidirectional radiation patterns a rectangular metallic cavity has been used. The design of the cavity is similar as that of cavity backed spiral antennas. The constructed cavity is filled with Eccosarb LS type absorbing materials of different grades to make the antenna to work over wide frequency band. Fig. 8 shows an illustration of the developed cavity backed antenna. The overall size of the cavity is $75 \times 60 \times 50$ mm. The disadvantage of using a cavity is that only half of the input power is transformed into radiated power because of the presence of the absorber which absorbs the radiation in that direction.

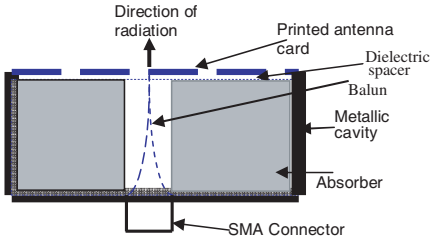

Figure 8. Schematic of antenna assembly showing its components.

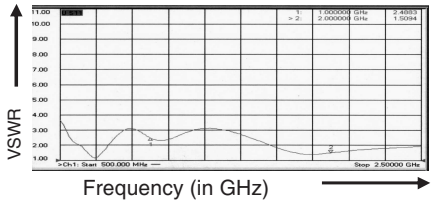

Figure 9. Measured VSWR of the antenna.

Three antenna models with different growth factors 1.2, 1.6 and 1.8 were printed on RT-duroid 5880 copper clad material keeping the optimized feed gap same. The antenna card was integrated with the cavity loaded with graded absorber. It was excited at the center feed point by twin wires (not shown in the assembly of Fig. 8) soldered to the broadband printed transformer. The printed transformer is passed through the center of the cavity and extends up to the back wall of the cavity. At the cavity base it is soldered to the center tab of the SMA coaxial connector. The connector flange is soldered to the balun ground plane. A 1 mm thick dielectric spacer is provided between the antenna card and the absorber in the cavity for providing mechanical rigidity and flatness to the thin 'printed card' (Fig. 8).

5. RESULTS AND DISCUSSIONS

The antenna having growth factor $g = 1.8$ (Fig. 7) was evaluated experimentally for its VSWR, radiation pattern and gain over the frequency band of 1 to 2 GHz. The swept frequency VSWR was measured on HP-8722D vector network analyzer. The VSWR plot versus frequency is shown in Fig. 9. The antenna has a VSWR less than 3 : 1 over the complete band. The antenna radiation patterns were measured in anechoic chamber using a Precision Network Analyzer (PNA) based automatic measurement set up. The radiation pattern E_θ cuts for $\phi = 0°$ and $\phi = 90°$ planes are shown in Figs. 10(a)–(f) for 1.0 GHz, 1.5 GHz and 2 GHz respectively. The patterns were plotted for both horizontal and vertical received polarizations. The measured axial ratio over the frequency band is shown in Fig. 11. From these measurements it is observed that the antenna has very low axial ratio ($< \pm 3$ dB) circular polarization characteristics over wide elevation angles. However, a commonly used criterion states that the axial ratio should be less than 6 dB [18]. The 3 dB beamwidth of the

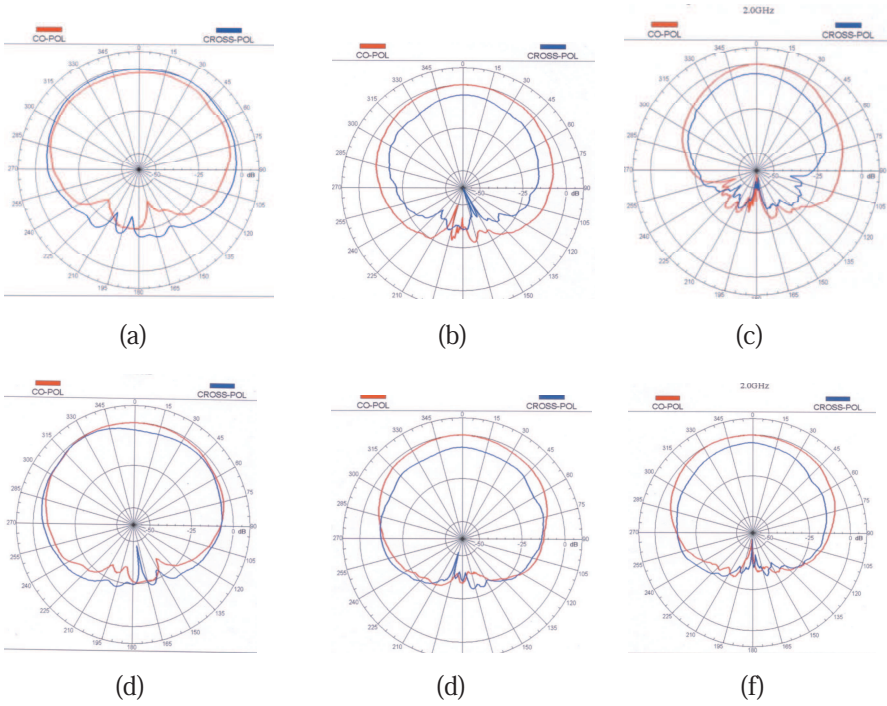

Figure 10. Measured radiation patterns of the antenna for $\phi = 0°$ and $\phi = 90°$ plane (VP — red; HP — blue). (a) Freq. 1 GHz for $\phi = 0°$, (b) Freq. 1.5 GHz for $\phi = 0°$, (c) Freq. 2 GHz for $\phi = 0°$, (d) Freq. 1 GHz for $\phi = 90°$, (e) Freq. 1.5 GHz for $\phi = 90°$, (f) Freq. 2 GHz for $\phi = 90°$.

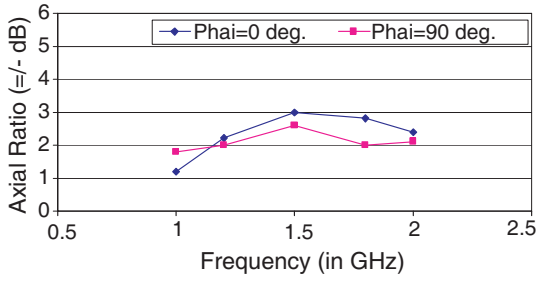

Figure 11. Measured axial ratio of the antenna for $\phi = 0°$ and $\phi = 90°$ plane.

antenna is measured to be better than 100° for all the frequencies. The antenna gain has been measured to be between −8 dB to −2 dB over the frequency band.

From the measurements, it is observed that the antenna VSWR is $\leq 3:1$ over the complete GNSS band. Its radiation characteristics show a very wide angle coverage which makes this antenna as one of the most suitable candidate for GNSS based LAAS system. The measured gain variation is less than 3 dB over ±50° from zenith and less than 6 dB covering ±80°. Hence, the antenna will be very effective in receiving the ranging signals in LAAS network from large number of satellites, available above the horizon at wider angular separation. Thus the GNSS receiver can provide higher degree of accuracy and integrity for aircraft navigation at and around the airport through corrections provided by augmentation systems. The axial ratio measured is ±2 dB more than the simulated results. This deviation may be due to factors which were not considered or modeled in analysis such as feed line 'balun' transformer, absorber filled cavity and anisotropy of dielectric material used for printing. The antenna has significantly low back lobe level of −25 dB at lower end of frequency which further decreases to −40 dB at higher end. The low back lobe is one of the important requirements from any GNSS antenna system for reduced interference signal reception from ground. This has been achieved due to use of absorber filled metallic cavity behind the antenna radiating element. In the absence of the cavity the antenna will have bidirectional radiation patterns as observed in simulation results. The antenna shows relatively low gain characteristics compared to patch antennas. However, its excellent circular polarization, wide angle coverage and wide frequency band operation makes it very useful antenna for GNSS based LAAS applications. Lower gain can be enhanced by integrating a Low Noise Amplifier (LNA) at the antenna output, before injecting the received signal to the receiver. The antenna is compact, lightweight and easily realizable. It can be made more compact in size by using a high dielectric substrate with some reduction in the gain.

6. CONCLUSION

A new cavity backed half-cardioid shaped dual arms; wide band printed circuit antenna has been successfully designed and developed. The antenna design parameters are analyzed and optimized initially with Finite element analysis tool. The extensive measurements of antenna characteristics show that it can effectively receive satellite signals from multi-constellation GNSS present over wide angles. The measured VSWR of the antenna is $< 3:1$. The antenna radiation patterns are

right hand circularly polarized with low axial ratio ($< \pm 3$ dB) covering 1 to 2 GHz frequency band. The antenna measured characteristics are in good agreement with the simulated results. With metallic cavity the antenna back lobe is very low. Also, the phase center of the antenna does not change with frequency. Thus, it can provide improved accuracy, availability and integrity necessary for all weather category II and III landing of aircraft in LAAS applications. The antenna can be easily fabricated, weighs less than 150 grams and is low in cost too. It will find extensive use in ground based, ship based or airborne platforms for GNSS signal reception.

ACKNOWLEDGMENT

The first and third authors sincerely acknowledge the encouragement and support given by Sri G Boopathy, Director, DLRL during the work and Dr. V. C. Misra, Director, Technologies for stimulus technical discussions during the development of the antenna. Thanks are also due to Smt. V. Sarla Devi for measurements on the antenna.

REFERENCES

1. Braff, R., "Description of the FAA's local area augmentation system (LAAS)," *Navigation, Journal of the Institute of Navigation*, Vol. 44, No. 4, 411–423, Winter 1997–1998.
2. Kovar, P., P. Puricer, P. Kacmarik, and F. Vejrazka, "Augmentation methods for GNSS integrity and precision enhancement in difficult environment," *Proceedings of TimeNav 07, ENC-GNSS, European Navigation Conference*, 107–114, The Printing House Inc., Stoughton, 2007.
3. Rizos, C., et al., "New GNSS developments and their impact on providers and users spatial information," (http://www.gmat.unsw.edu.au/snap/publications/rizosetal 2005a.pdf).
4. Constantinescu, A. and R. J. Landry, "GPS/Galileo/GLONASS hybrid satellite constellation simulator — GPS constellation validation analysis," *The Institute of Navigation 61st Annual Meeting*, 733–737, Cambridge, MA, USA, 2005.
5. Zhang, Y. and H. T. Hui, "A printed hemispherical helical antenna for GPS receivers," *IEEE Microwave and Wireless Components Letters*, Vol. 15, No. 1, 10–12, Jan. 2005.
6. Baik, J. W., K. J. Lee, W. S. Yoon, T. H. Lee, and Y. S. Kim, "Circularly polarised printed crossed dipole antennas

with broadband axial ratio," *Electronics Letters*, Vol. 44, No. 13, 785–786, Jun. 19, 2008.

7. James, J. R. and P. S. Hall, *Handbook of Microstrip Antennas*, Peter Perigrinus Ltd., London, 1989.
8. Padros, N., et al., "Comparative study of high-performance GPS receiving antenna designs," *IEEE Trans. Antennas and Propagation*, Vol. 45, No. 4, 698–706, Apr. 1997.
9. Pozar, D. M. and S. M. Duffy, "A dual-band circularly polarised aperture-coupled stacked microstrip antenna for global positioning system," *IEEE Trans. Antennas and Propagation*, Vol. 45, No. 11, 1618–1625, Nov. 1997.
10. Boccia, L., et al., "A high performance dual frequency microstrip antenna for global positioning system," *IEEE Antenna and Propagation Soc. Int. Symposium*, Vol. 4, 66–69, 2001.
11. Rao, B. R., et al., "Triple band GPS trap loaded inverted L antenna array," *Microwave and Optical Technology Letters*, Vol. 38, No. 1, 25–37, 2003.
12. Yang, F. and Y. Rahamat-Samii, "A single layer dual band circularly polarized microstrip antenna for GPS applications," *IEEE Antennas and Propagation Society International Symposium*, Vol. 4, 720–723, Jun. 2002.
13. Zhou, Y., C.-C. Chen, and J. L. Volakis, "Proximity-coupled stacked patch antenna for tri-band GPS applications," *IEEE Antennas and Propagation Society International Symposium 2006*, 2683–2686, Jul. 9–14, 2006.
14. DuHamel, R. H. and D. E. Isbell, "Broadband logarithmically periodic antenna structures," *IRE National Convention Record*, No. 1, 1957.
15. Rumsey, V. H., "Frequency-independent antennas," *IRE National Convention Record*, Vol. 5, Part 1, 114–118, 1957.
16. Grewal, B. S., *Higher Engineering Mathematics*, 36th edition, Khanna Publications, New Delhi, 1998.
17. Dyson, J. D., "The equiangular spiral antenna," *IRE Transactions on Antennas and Propagation*, 181–187, 1959.
18. Thaysen, J., et al., "Numerical and experimental investigation of a coplanar waveguide-fed spiral antenna," *IEEE 24th QMW Antenna Symposium*, 13–16, 2000.
19. High-frequency Structure Simulator (HFSS V10.1) software from Ansoft Corp. (Pittsburgh, PA).